A first principles study on tunneling current through Si/SiO2/Si structures

Yamada, Yoshihiro
Tsuchiya, Hideaki
Ogawa, Matsuto

(Citation)
Journal of Applied Physics,105(8):083702-083702

(Issue Date)
2009-04-17

(Resource Type)
journal article

(Version)
Version of Record

(URL)
https://hdl.handle.net/20.500.14094/90000912

A first principles study on tunneling current through $Si/SiO_2/Si$ structures

Y. Yamada, H. Tsuchiya,[a] and M. Ogawa
Department of Electrical and Electronics Engineering, Graduate School of Engineering, Kobe University, 1-1, Rokko-dai, Nada-ku, Kobe 657-8501, Japan

(Received 6 October 2008; accepted 21 February 2009; published online 17 April 2009)

In this paper, we study tunneling current properties through SiO_2 gate oxides in Si metal-oxide-semiconductor field-effect transistors (MOSFETs) by applying a first principles method based on the density-functional theory and nonequilibrium Green's function approach. We employed three structural models of SiO_2 layers, which are β-quartz, β-cristobalite, and β-tridymite. As a result, we found that the β-cristobalite and β-tridymite models indicate similar tunneling current properties, while the β-quartz model predicts a substantially lower tunneling current. Further, the largest tunneling current is obtained for the β-tridymite SiO_2 model, which is consistent with bandstructure parameters estimated for bulk SiO_2 crystals. Therefore, electronic properties of bulk SiO_2 crystals can still be important for tunneling current analysis in the nanoscale range of oxide thickness.
 [DOI: 10.1063/1.3106115]

I. INTRODUCTION

Today's very-large-scale integrated circuit (VLSI) technology requires an atomic-scale understanding of physical phenomena arising from the miniaturization of Si metal-oxide-semiconductor field-effect transistors (MOSFETs). One of the most important technological roadblocks for further miniaturization is the high quantum mechanical tunneling current through the gate oxide, which greatly increases VLSI power consumption. Therefore, an accurate modeling of tunneling current through the ultrathin SiO_2 gate oxide[1,2] and an alternative high-k gate oxide[3] is currently of utmost importance for device design.

So far, an atomistic formalism based on the empirical tight-binding (TB) method, embedded in a transfer matrix scheme,[1] has been applied to calculate tunneling current through three structural models of SiO_2 layers, which are β-cristobalite, β-quartz, and β-tridymite.[2] Then, the TB approach showed that the β-cristobalite model gives the largest tunneling current for a wide range of the oxide thickness from sub-1 to 5 nm, and consequently the best agreement with experimental results[4] was obtained for the β-cristobalite model. On the other hand, the β-cristobalite phase on Si (001) surface has been reported to be unstable because of large lattice mismatch at the Si/SiO_2 interface, and transforms into a highly distorted structure.[5] Hence, in this paper we examine the influence of the microscopic oxide structure on gate tunneling current properties by using a fully first principles approach.

In the present approach, tunneling probabilities through SiO_2 layers are calculated using the linear combination of atomic orbitals basis ATK code,[6,7] which is based on the density-functional theory (DFT) and the nonequilibrium Green's function method. Although the DFT theory is known to underestimate bandgaps significantly, the conduction band dispersions are reproduced accurately and thus transport parameters such as the conduction band effective mass are reliable. To overcome the bandgap shortcoming, new density functional methods, such as "sX-LDA (local density approximation)" employing screened nonlocal exchange and LDA correction potentials within DFT,[8] "EXX (exact exchange) potential method" allowing the determination of the exact Kohn–Sham exchange potential,[9,10] and "SIC method" introducing the self-interaction corrections,[11] and furthermore a first principles many-body theory of quasiparticle energies using the GW approximation,[12,13] have been presented in the literature whose bandgaps generally agree much better with experiment than the standard DFT method. Such an exact description of excited states in solids is a challenging and important problem in solid-state physics but it is still difficult to apply them to transport problems in nanoscaled structures due to the requirement of huge computational resources. Accordingly, we employed the standard DFT method with the generalized gradient approximation (GGA) exchange-correlation functionals to investigate the gate tunneling properties of SiO_2 gate oxides in this study.

II. THEORETICAL MODELS

Following Ref. 2, we adopted three crystalline models of SiO_2 gate oxide as shown in Fig. 1, where (a) is for β-quartz, (b) is for β-cristobalite, and (c) is for β-tridymite. In this study, we attempted to connect the SiO_2 layers to Si (001) surface by rotating the SiO_2 crystals so that the lattice constant closest to 5.43 Å of bulk Si crystal can be obtained. As a consequence, the interlayer SiO_2 crystals should be distorted in shape different from their equilibrium structures as follows. For β-quartz and β-cristobalite, they need to be biaxially tensiled in the plane perpendicular to $\langle 001 \rangle$ direction and compressed in $\langle 001 \rangle$ direction, and vice versa for β-tridymite. We first obtained such strained SiO_2 crystals by applying structural optimization procedures where a conjugate gradients minimization method was employed to relax all atomic coordinates and cell shape and size. Then, Si and O atoms at the Si/SiO_2 interfaces are bonded not to appear

[a]Author to whom correspondence should be addressed. Electronic mail: tsuchiya@eedept.kobe-u.ac.jp. Tel./FAX: +81-78-803-6082.

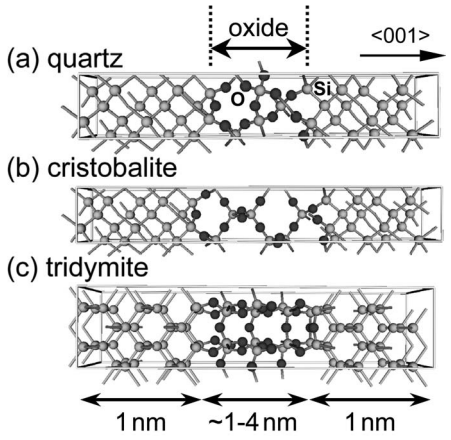

FIG. 1. Three atomic models of $Si(001)/SiO_2/Si(001)$ structures used in the simulation, where (a) β-quartz, (b) β-cristobalite, and (c) β-tridymite SiO_2 models.

any defects, as shown in Fig. 1. Here, we adopted a simpler interface structure for the β-cristobalite model than that in Ref. 2, in order for the width of the transition region to be minimized. In practice, the transition region of the β-cristobalite model was constructed in the same way as in the β-quartz model. Subsequently, the structural optimization procedures were again applied for all atoms in the SiO_2 layer and Si atoms neighboring the interfaces. Si atoms locating away from the interfaces were fixed at the equilibrium positions. For simplicity, the structural optimization procedures were performed only for zero bias condition, and thus a structural change due to the applied bias voltage is not considered here. In addition, a periodical boundary condition was employed at the ends of the left and right boundaries. The oxide thickness T_{SiO_2} is defined as a distance between Si atoms residing at the two surfaces.

As described in the Sec. I, tunneling probabilities were first calculated by using the linear combination of atomic orbitals basis ATK code,[6,7] where we used the GGA exchange-correlation functionals of Perdew, Burke, and Ernzerhof, and core electrons of atoms are represented by norm-conserving pseudopotentials with the Troullier–Martins parameterization. Next, tunneling current densities were estimated by using the Laudauer–Büttiker formulation with the calculated tunneling probabilities and the Fermi–Dirac distribution functions of n^+-Si and p-Si electrodes. The Fermi energies are given as $E_F \cong 150$ meV above the conduction band edge in n^+-Si electrode and $E_F \cong 240$ meV above the valence band edge in p-Si electrode, which correspond to background charge concentrations of 3×10^{20} and 1×10^{15} cm^{-3}, respectively.[2] Furthermore, only the negative gate bias is considered in the calculations to meet the same condition in Ref. 2.

III. RESULTS

First, Fig. 2 shows the oxide thickness dependences of current-voltage characteristics computed for (a) β-quartz, (b) β-cristobalite, and (c) β-tridymite. As expected, the tunneling current increases exponentially as T_{SiO_2} decreases. Here, it should be noted that tunneling current is almost constant

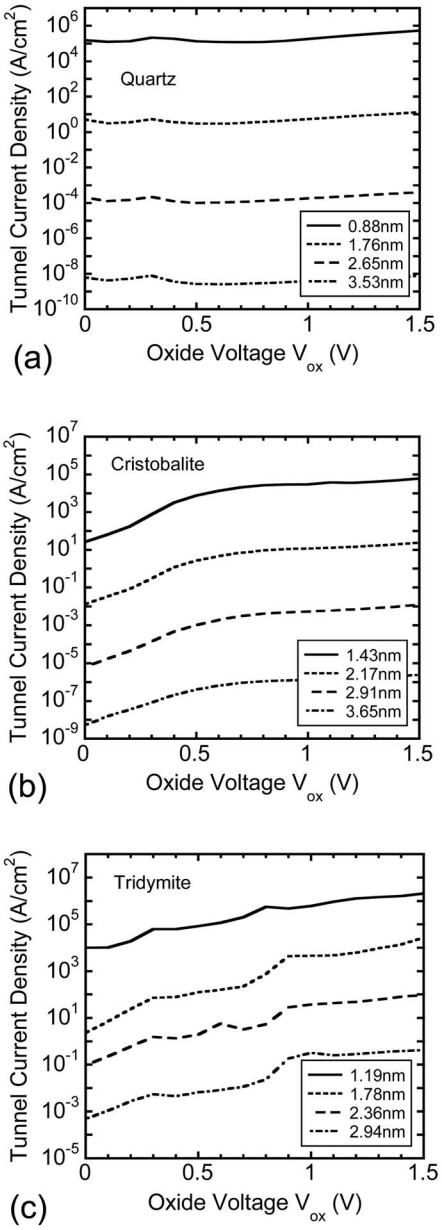

FIG. 2. Oxide thickness dependences of current-voltage characteristics computed for (a) β-quartz, (b) β-cristobalite, and (c) β-tridymite.

with the oxide voltage in the β-quartz model, whose behavior is obviously different from the experimental results.[4] There may be interesting physics behind this but it is still puzzling and under investigation. On the other hand, the β-cristobalite and β-tridymite models show the increase in the tunneling current with the oxide voltage, which are similar current-voltage characteristics to the experimental one, though numerical fluctuations are observed in the β-tridymite model. A reason for the fluctuations may be due to some technical difficulties in optimizing large atomic system. In other words, since the β-tridymite model has the highest atomic density among the three SiO_2 models and there exists a large compressive strain in the plane perpendicular to the current direction, it is likely hard to obtain a sufficiently relaxed $Si/SiO_2/Si$ structure.

As discussed in Ref. 2, the tunneling currents under negative gate bias consist of three main contributions, which

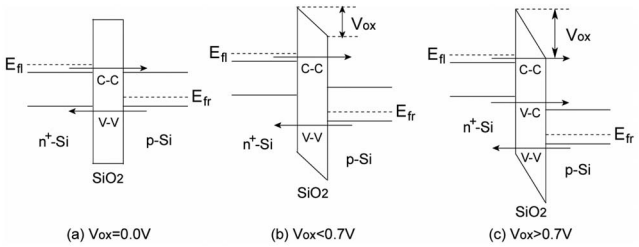

FIG. 3. Conduction- and valence-band diagrams of n^+-Si/SiO_2/p-Si structures for (a) $V_{ox}=0$ V, (b) $V_{ox}<0.7$ V, and (c) $V_{ox}>0.7$ V. *C-C* represents the direct tunneling of conduction band electrons from gate to substrate, *V-V* the tunneling due to valence band holes from substrate to gate, and *V-C* the tunneling due to electrons from valence band of gate to conduction band of substrate, which emerges as oxide voltage V_{ox} increases larger than Si bandgap energy (0.7 eV).

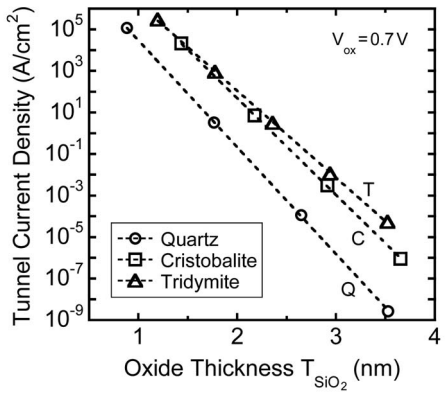

FIG. 5. Oxide thickness dependences of tunneling current density at $V_{ox}=0.7$ V, where the tunneling current is determined by the *C-C* component.

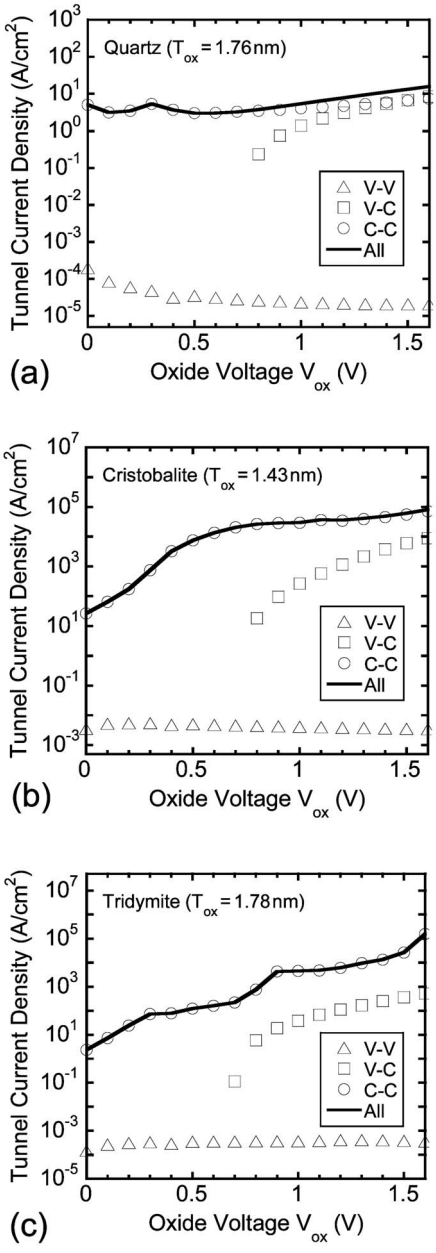

FIG. 4. Three tunneling current components, *C-C*, *V-V*, and *V-C*, computed for (a) β-quartz, (b) β-cristobalite, and (c) β-tridymite. The oxide thicknesses used in the calculation are indicated in each figure.

are schematically depicted in Fig. 3. One is direct tunneling of conduction band electrons from the gate to the substrate (*C-C*), which gives the most important contribution. The second one is due to valence band holes from the substrate to the gate (*V-V*), and the third one due to electrons from the valence band of the gate to the conduction band of the substrate (*V-C*), which emerges as the oxide voltage increases larger than the Si bandgap energy as shown in Fig. 3(c), where the bandgap energy of bulk Si was estimated to be 0.7 eV from our bandstructure calculations, which is quite smaller than 1.2 eV of Ref. 2 due to the DFT/GGA formalism. These three components are separately plotted in Fig. 4 for the three SiO_2 models, where the oxide thicknesses used in the calculation are indicated in each figure. The *V-V* component, that is hole current, is negligible due to higher Si/SiO_2 valence band offset.[2] The *C-C* component is dominant as expected, but the *V-C* component becomes comparable to the *C-C* contribution for $V_{ox}>0.7$ V. As shown in Fig. 4(a), the *V-C* contribution in the β-quartz model is excessive, so the β-quartz model indeed has different tunneling properties from the other models. Incidentally, the *C-C* and *V-V* currents flow at $V_{ox}=0$ V because the Fermi energies between n^+-Si and p-Si electrodes are different as shown in Fig. 3(a).

Next, Fig. 5 shows the tunneling current density as a function of the oxide thickness at $V_{ox}=0.7$ V, where the tunneling current densities are determined by the *C-C* component, as shown in Fig. 4. It is found that the β-cristobalite and β-tridymite models have similar current-thickness properties, while the β-quartz model gives at least two orders of magnitude lower current density. The present results are basically consistent with the previous results based on the TB formalism, where the lower tunneling current in the β-quartz model was plausibly explained using its largest conduction band effective mass.[2] Therefore, we further examined the bandstructure parameters for bulk SiO_2 crystals. Figure 6 shows the computed bandstructures along the tunneling current direction ⟨001⟩ for (a) β-quartz, (b) β-cristobalite, and (c) β-tridymite crystals. The length of the first-Brillouin zone is different among the three SiO_2 crystals because each SiO_2 crystal has a different unit cell size along the current direction as $a_q=0.88$ nm (β-quartz), $a_c=0.74$ nm (β-

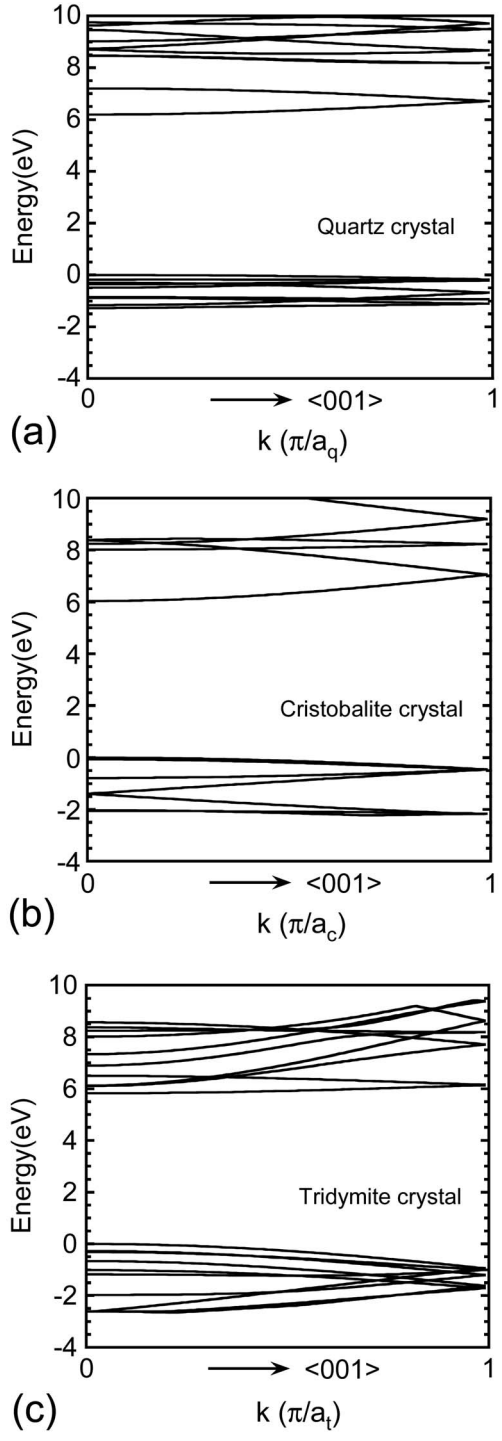

FIG. 6. Computed bandstructures along tunneling current direction ⟨001⟩ for (a) bulk β-quartz, (b) bulk β-cristobalite, and (c) bulk β-tridymite crystals, where SiO_2 lattice constants were taken as the same values as in $Si/SiO_2/Si$ structures shown in Fig. 1. Each crystal has a different unit cell size as a_q =0.88 nm, a_c=0.74 nm, and a_t=0.56 nm for the β-quartz, β-cristobalite, and β-tridymite crystals, respectively.

cristobalite), and a_t=0.56 nm (β-tridymite). It is found in Fig. 6 that the conduction band minimum is located at the Γ point (k=0) and the valence band width is very narrow, which had been already reported by several authors.[14,15] Such overall characteristics are similar among the three SiO_2 crystals but the detailed bandstructure parameters at the Γ point depend on the SiO_2 crystals as summarized in Table I,

TABLE I. Conduction band effective masses and bandgap energies extracted from the bandstructure calculations for the bulk SiO_2 crystals.

	Quartz	Cristobalite	Tridymite
Conduction band mass (m_0)	0.77	0.56	0.30
Bandgap energy (eV)	6.19	6.03	5.82

where the effective masses at the conduction band minimum and bandgap energies are compared. Although the DFT/GGA formalism underestimates the bandgap energies considerably, compared with the experimental one (~9.0 V), the conduction band dispersions are reproduced accurately and the estimated conduction band masses are reliable. According to Table I, the largest values in both the conduction band masses and bandgap energies are obtained for the bulk β-quartz crystal, while the smallest values are obtained for the bulk β-tridymite crystal. These results are in reasonable agreement with the magnitude of tunneling current densities shown in Fig. 5.

To understand correlations between the magnitude relation of the tunneling current densities in Fig. 5 and the bandstructure parameters of the SiO_2 crystals in Table I, we calculated the current-oxide thickness dependences corresponding to the C-C component by using the bandstructure parameters of Table I, based on the conventional transfer-matrix method. In the transfer-matrix calculation, the conduction band discontinuity energy ΔE_C was simply given by $\Delta E_C=[E_G^{ox}(\mathrm{DFT})-E_G^{Si}(\mathrm{DFT})]/2$, where $E_G^{ox}(\mathrm{DFT})$ and $E_G^{Si}(\mathrm{DFT})$ are bandgap energies calculated for the bulk SiO_2 and Si crystals based on the present DFT approach. The results are plotted in Fig. 7, which represents that the same magnitude relation among the three oxide structures as those in Fig. 5 is obtained, though difference between the β-cristobalite and β-tridymite models is estimated to be larger. To further analyze if the difference in the tunneling current densities is more due to the different effective masses or due to the different bandgaps, we also calculated the current-oxide thickness dependences by altering only effective mass or bandgap energy, as shown in Fig. 8, where (a) bandgap energy and (b) effective mass are fixed at the values of the β-quartz crystal, respectively. From Figs. 7 and 8, we

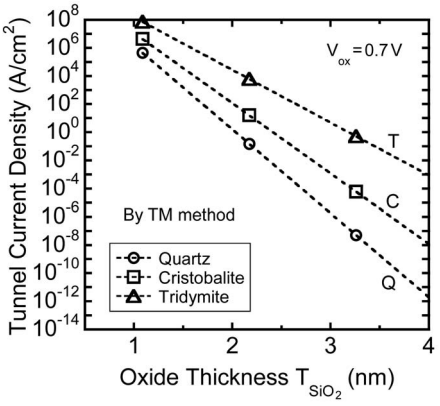

FIG. 7. Oxide thickness dependences of tunneling current density at V_{ox} =0.7 V, computed by using a transfer-matrix method with effective masses and bandgap energies of Table I.

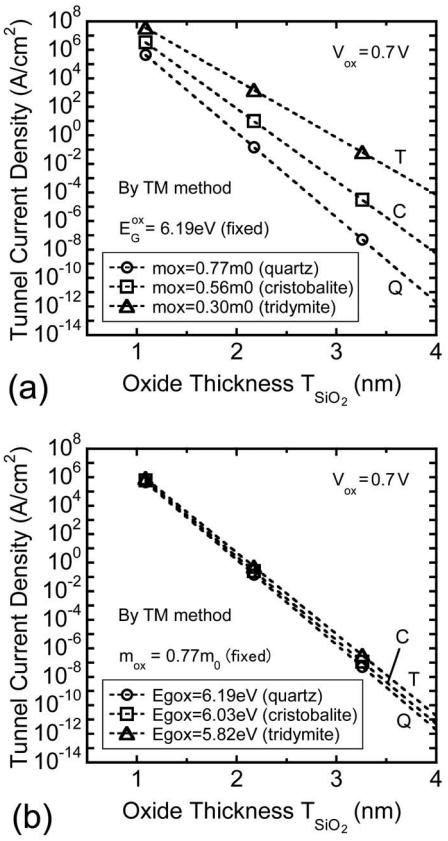

FIG. 8. Oxide thickness dependences of tunneling current density at V_{ox} =0.7 V, computed by using the transfer-matrix method with altered only (a) effective mass and (b) bandgap energy, where (a) bandgap energy and (b) effective mass are fixed at the value of β-quartz crystal, respectively.

can conclude that the tunneling current densities are more sensitive to the difference in the conduction band effective masses than that in the bandgaps. In addition, the small discrepancy between the β-cristobalite and β-tridymite models observed in Fig. 5 suggests a possibility of reconstruction of the SiO_2 atomic structures in the presence of the Si/SiO_2 interfaces. Nevertheless, the above results mean that the electronic properties of bulk SiO_2 crystals can still be important for the tunneling current behaviors even in the nanoscaled SiO_2 gate oxides.

IV. CONCLUSION

We have investigated tunneling current properties through $Si/SiO_2/Si$ structures based on first principles simulation. As a result, we found that the β-cristobalite and β-tridymite models have similar tunneling current properties but the β-quartz model represents a substantially lower tunneling current. We also observed that the largest tunneling current is obtained for the β-tridymite SiO_2 model, which is consistent with conduction band effective masses and bandgap energies estimated for bulk SiO_2 crystals. Therefore, electronic properties of bulk SiO_2 gate oxides, especially the conduction band effective mass, will be still important for tunneling current analysis in the nanoscale range of the oxide thickness. For direct comparison of the calculated tunneling currents with experimental values, more advanced theoretical treatment for the exchange-correlation functionals such as EXX and SIC methods will be necessary.

ACKNOWLEDGMENTS

This work was partially supported by a NEDO/MIRAI project.

[1]M. Städele, B. R. Tuttle, and K. Hess, J. Appl. Phys. **89**, 348 (2001).
[2]F. Sacconi, A. D. Carlo, P. Lugli, M. Städele, and J.-M. Jancu, IEEE Trans. Electron Devices **51**, 741 (2004).
[3]F. Sacconi, J.-M. Jancu, M. Povolotskyi, and A. D. Carlo, IEEE Trans. Electron Devices **54**, 3168 (2007).
[4]Khairurrijal, W. Mizubayashi, S. Miyazaki, and M. Hirose, J. Appl. Phys. **87**, 3000 (2000).
[5]T. Yamasaki, C. Kaneta, T. Uchiyama, T. Uda, and K. Terakura, Phys. Rev. B **63**, 115314 (2001).
[6]J. M. Soler, E. Artacho, J. D. Gale, A. García, J. Junquera, P. Ordejón, and D. Sánchez-Portal, J. Phys.: Condens. Matter **14**, 2745 (2002).
[7]M. Brandbyge, J.-L. Mozos, P. Ordejón, J. Taylor, and K. Stokbro, Phys. Rev. B **65**, 165401 (2002).
[8]A. Seidl, A. Gorling, P. Vogl, and J. A. Majewski, Phys. Rev. B **53**, 3764 (1996).
[9]T. Kotani and H. Akai, Phys. Rev. B **52**, 17153 (1995).
[10]M. Städele, J. A. Majewski, and P. Vogl, Phys. Rev. Lett. **79**, 2089 (1997).
[11]J. P. Perdew and A. Zunger, Phys. Rev. B **23**, 5048 (1981).
[12]L. Hedin, Phys. Rev. **139**, A796 (1965).
[13]M. S. Hybertsen and S. G. Louie, Phys. Rev. B **34**, 5390 (1986).
[14]E. Gnani, S. Reggiani, R. Colle, and M. Rudan, IEEE Trans. Electron Devices **47**, 1795 (2000).
[15]Y. Xu and W. Y. Ching, Phys. Rev. B **44**, 11048 (1991).